ORGANOGENESIS
2021, VOL. 17, NOS. 3–4, 56–71
https://doi.org/10.1080/15476278.2021.1954769

Taylor & Francis
Taylor & Francis Group

RESEARCH PAPER

Osteogenic and Angiogenic Synergy of Human Adipose Stem Cells and Human Umbilical Vein Endothelial Cells Cocultured in a Modified Perfusion Bioreactor

Fatemeh Mokhtari-Jafari[a,b], Ghasem Amoabediny[a,b], Mohammad Mehdi Dehghan[c,d], Sonia Abbasi Ravasjani[b,e], Massoumeh Jabbari Fakhr[c,d], and Yasaman Zamani[b,e]

[a]School of Chemical Engineering, College of Engineering, University of Tehran, Tehran, Iran; [b]Department of Biomedical Engineering, Research Center for New Technologies in Life Science Engineering, University of Tehran, Tehran, Iran; [c]Department of Surgery and Radiology, Faculty of Veterinary Medicine, University of Tehran, Tehran, Iran; [d]Institute of Biomedical Research, University of Tehran, Tehran, Iran; [e]Department of Biomedical Engineering, Faculty of New Sciences and Technologies, University of Tehran, Tehran, Iran

ABSTRACT

Synergistic promotion of angiogenesis and osteogenesis in bone tissue-engineered constructs remains a crucial clinical challenge, which might be overcome by simultaneous employment of superior techniques including coculture systems, differentiation-stimulated factors, combinatorial scaffolds and bioreactors.

Current study investigated the effect of flow perfusion along with coculture of human adipose stem cells (hASCs) and human umbilical vein endothelial cells (HUVECs) on osteogenic and angiogenic differentiation.

Pre-treated hASCs with 1,25-dihydroxyvitamin D_3 were seeded onto poly(lactic-co-glycolic acid)/β-tricalcium phosphate/polycaprolactone (PLGA/β-TCP/PCL) scaffold with/without HUVECs, and cultured for 14 days within a flask or modified perfusion bioreactor. Analysis of osteogenic and angiogenic gene expression, alkaline phosphatase (ALP) activity and ALP staining indicates a synergistic effect of perfusion flow and coculture system on osteogenic and angiogenic differentiation. The advantage of modified perfusion bioreactor is its five-branch flow distributor which directly connect to the porous PCL hollow fibers embedded in the 3D scaffold to improve flow and flow-induced shear stress uniformity.

Dynamic coculture increased $VEGF_{165}$ by 6-fold, $VEGF_{189}$ by 2-fold, and Endothelin-1 by 4-fold, relative to dynamic monoculture. Static coculture enhanced osteogenic and angiogenic differentiation, compared with static monoculture. Although dynamic coculture is in preference to static coculture due to significant increase in ALP activity and promoted angiogenic marker expression. Our finding is the first to indicate that the modified perfusion bioreactor combined with the beneficial cell-cell crosstalk in pre-treated hASC/HUVEC cocultures provides a synergy between osteogenic and angiogenic differentiation of the accumulation of cells, suggesting that it represents a promising approach for regeneration of critical-sized bone defects.

ARTICLE HISTORY
Received 27 March 2020
Revised 24 May 2020
Accepted 8 July 2020

KEYWORDS
bone; osteogenic differentiation; angiogenic differentiation; human umbilical vein endothelial cells; human adipose stem cells; modified perfusion bioreactor

INTRODUCTION

It is a great challenge to prepare "vascularized functional artificial bone" for the repair of large segmental defect, especially in weight-bearing bones.[1] It is obvious that the success of prevascularization depends on multiple factors, including source of cells, differentiation-stimulated factors, and tissue engineering environment such as the biomaterials, structure of scaffolds, and bioreactors. Over the past decade, scaffold design remains a challenge in tissue engineering due to the large number of requirements that need to be met, such as having the ability to deliver cells, supporting differentiation of regenerative cells, irregular geometries, biocompatibility, osteoconductivity and osteoinductivity.[2]

Scaffolds with aligned microchannels regulate *in vitro* cell activities, and enhance cell infiltration and vascularization upon *in vivo* implantation which result the desired construct with functional integration and better repair capacity.[3] 3D structures containing porous hollow fibers for nutrition delivery can be suitable for *in vitro* bioreactors studies for production of tissue-engineered constructs or *in vivo* prepared bone grafts.[4] Synergistic approach of incorporating osteoconductive nanomaterials built on

CONTACT Ghasem Amoabediny amoabediny@ut.ac.ir School of Chemical Engineering, College of Engineering, University of Tehran, Tehran, Iran
Supplemental data for this article can be accessed on the publisher's website.

a biomaterial scaffold which is hydrophilic, biocompatible, and specifically incorporated with biochemical cues can direct bone regeneration.[5] The material properties of scaffold have a strong effect on the mechanical strength of final construct, especially when they are subjected to tensile and compressive stresses.[6] Since calcium phosphate-based materials direct stem cell differentiation toward osteolineage cells, and PLGA as a hydrophilic material serve as a platform for bone tissue regeneration,[5] β-TCP and PLGA were used as the biomaterials of 3D porous scaffold in this study. MSCs play fundamental roles as promoters, enhancers, and playmakers of the translational regenerative medicine which the most reported translational use of MSC therapy is related to bone tissue regeneration.[7] Mesenchymal stem cells (MSCs) derived from bone marrow, adipose tissue, or umbilical cords can be used as vascularization units and considered as building blocks for tissue engineering due to increased angiogenic and vasculogenic potential.[8] The capability of MSCs to differentiate into several cell types, as well as their important immunomodulatory effects, support self-regulated healing processes in damaged tissues.[9] Osteogenic differentiation potential of oral derived MSCs (human periapical cyst MSCs) along with secretion of several immunomodulatory molecules provide a regenerative microenvironment.[9] Oral-derived MSCs such as human periodontal ligament stem cells may be appropriate for angiogenesis. Endothelial differentiation of human periodontal ligament stem cells leads the cells to respond to lipopolysaccharide derived from porphyromonas gingivalis activating reactive oxygen species (ROS) production as an important signaling molecule that regulate multiple biological responses, including angiogenesis.[10]

MSCs have the ability to differentiate into osteoprogenitors and osteoblasts as well as to form calcified bone matrix.[11] The potential of hASCs as a rich source of MSCs to stimulate osteogenesis and angiogenesis holds interesting promises to the field of bone tissue engineering.[12] hASCs are more efficient in both *in vitro* and *in vivo* angiogenesis promotion than umbilical cord and endometrium tissues due to secreting more proangiogenic cytokines and less inhibitor.[13] Apart from multilineage differentiation potential, hASCs have attracted much attention due to strong proliferation and migration abilities *in vitro* and high resistance to oxidative stress and senescence.[14] Adipose stem cells (ASCs) seeding on TCP-PLGA scaffolds improves bone regeneration in large mandibular defects, although further improvement with regard to the osteogenic and neo-angiogenic capacity is required to transfer this concept into clinical use.[15]

Synergistic promotion of HUVEC angiogenesis and human MSC osteogenesis cocultured statically on a nanomatrix[16] or calcium phosphate cement scaffold[17] has been demonstrated. Coculture of human-induced pluripotent stem cell-derived MSCs and HUVECs enhances the formation of capillary-like structures, osteogenesis and mineralization within the scaffold.[17] To achieve a synergism between osteogenic and angiogenic differentiation capacity and chemoattractive potential, a combination of adipose tissue, platelets and cell culture supernatants appears promising for potential clinical applications.[18]

HUVEC and bone marrow MSCs (BMSCs) cocultures enhance vascularization in critical-sized cranial defects in a time-dependent manner; in which after 2 weeks of culture, 70% MSC have the highest vessel length and endothelial cell network area than other proportions, and after 3 weeks, 50% MSC group is more vasculogenic than other proportions.[19] Along with vasculogenesis and angiogenesis, mineralization is also required to enhance the utility of construct for bone tissue-engineering applications; coculture of primary human endothelial cells and bone-derived osteoblasts in ratios of 5:1 improves vasculogenesis, but the 1:5 direct coculture ratio results in most mineralization to improve bone formation.[20] Endothelial cells can form viable, circular, and stable spheroids when combined with supporting cells (human foreskin fibroblasts, hASCs) in a 1/9 cell ratio.[21] Inspired by previous studies, in the current study, HUVECs and hASCs were mixed in a proportion of 1:2.5 (almost 70% hASCs) to bring the benefits of angiogenic and osteogenic synergy of the accumulation of cells.

The observation of bone formation at a bone defect site of chick using coculture of BMSCs and HUVECs has highlighted the efficacy of coculture systems as an inexpensive, high-throughput *ex vivo* model for preliminary research.[22] Comparable results have shown that local injection of BMSCs

or ASCs can induce a significant improvement in bone healing.[23] Since human BMSCs requires an invasive procedure to harvest, other cell sources of MSCs such as hASCs could also serve as a valuable alternative to BMSCs with similar osteogenic and angiogenic capacity *in vitro* and *in vivo*.[24] Coculture of hASCs and HUVECs on PCL/gelatin nanofiber scaffolds generates a mature blood-vessel -like network and increases the expression of tight junction proteins compared with monocultured HUVECs.[25]

Cellular mechanism of angiogenesis in both endothelial cells (ECs) and ASCs are still heavily debated. Angiogenesis in a 3D model containing adipose tissue stem cells and ECs is mediated by canonical Wnt signaling.[26] Coculture of endothelial progenitor cells and MSCs enhanced their proliferation and angiogenesis through PDGF and Notch signaling.[27] Silencing Schnurri-3 as a critical mediator of postnatal bone formation could dramatically enhance the expression of Runx2, which directly regulates the downstream target VEGF to couple osteogenic differentiation with angiogenesis.[28] Interestingly, the exosomes secreted by endothelial progenitor cells in stimulating angiogenesis is closely coupled with osteogenesis and accelerate bone regeneration during distraction osteogenesis.[29]

Apart from coculture systems, mechanotransduction can also stimulate osteogenesis independently of other environmental factors.[30] A recent study has reported that bioreactor-based preconditioning augments the bone-forming potential of bone marrow aspirate.[31]

Dynamic culture of BMSC and HUVEC in a tubular perfusion bioreactor has further augmented gene expression of alkaline phosphatase (ALP), bone morphogenetic protein 2 (BMP-2), vascular endothelial growth factor (VEGF), PECAM (platelet endothelial cell adhesion molecule) compared with static coculture, indicating a synergistic effect between coculture and applied shear stress.[32] Perfusion bioreactor with flow rate of 1 to 5 mL/min improves nutrient exchange and waste removal, resulting in increased cell viability, while cyclic compression loading at frequencies of 0.5 to 5 Hz enhances extracellular matrix (ECM) mineralization.[33] It has been also reported that continuous perfusion cultures at flow rate of 1 ml/min support osteogenic differentiation and ECM formation of hASCs in a macroporous ceramic scaffold.[34] Dynamic MSCs culture increases expression of osteoblastic marker genes even under physiological level of low fluid flow-induced shear stress (0.012–0.015 Pa).[35]

Tubular perfusion bioreactor provides long-term shear stresses on osteoblastic differentiation of hMSCs, in which flow rate of 3 ml/min is preferable to 10 ml/min, because both 3 and 10 mL/min flow rate stimulated the osteoblastic differentiation of the cells, but alginate scaffold dissolution in 3 ml/min does not occur too quickly.[36] Since degradation of PLGA/β-TCP scaffolds under dynamic conditions exhibited a significantly faster rate than that under static conditions,[37] in the current study, flow rate of 3 ml/min was selected for the modified perfusion bioreactor, in which a five-branch flow distributor evenly distributes culture medium within the 3D scaffold.

Since differentiation-stimulated factors and ECs both play active roles in bone regeneration, a recent study has compared the effects of both BMP-2 and HUVECs and showed both factors significantly promotes the osteogenic potential of MSCs *in vitro*, although BMP-2 displayed a significantly faster effect than HUVECs.[38] The use of safe, quality-controlled, and potentially advantageous supplements such as human-platelet lysate instead of fetal bovine serum in culture medium could establish clinical-grade protocols for regenerative medicine applications.[39] The osteogenic markers including ALP, osteopontin, and osteocalcin were increased by 25-hydroxyvitamin D_3 and 1α,25-dihydroxyvitamin D_3 (1,25-$(OH)_2$VitD_3) in a dose-dependent manner in which 10 nM 1,25-$(OH)_2D_3$ increased ALP activity and osteogenic differentiation more than 0.05, 0.1 and 1 nM.[40] In addition, 30 min pretreatment with physiological concentration (10 nM) of 1,25-$(OH)_2$VitD_3 is far superior to continuous treatment in stimulating osteogenic differentiation of hASCs.[41] Based on our previous reported data,[41] we treated hASCs with 1,25-$(OH)_2$VitD_3 before coculture with HUVEC to evaluate osteogenesis and

angiogenesis of the accumulation of cells in the current study.

Therefore, we tested the effect of flow perfusion culture on osteogenic and angiogenic differentiation of hASCs and HUVECs coculture, which has considerable potential for bone tissue regeneration. Moreover, we compared the potency of dynamic coculture for symbiotic relationship between osteogenic and angiogenic differentiation, to static and dynamic monoculture.

METHODS

PLGA/β-TCP/PCL Scaffold

The porous cylindrical poly(lactic-co-glycolic acid)/β-tricalcium phosphate (PLGA/β-TCP) scaffold employed in this study has a diameter of 22 mm and a height of 10 mm which five blind end polycaprolactone (PCL) porous hollow fibers were embedded in the scaffold (PLGA/β-TCP /PCL). Inner diameter of the PCL porous hollow fibers was 2 mm and the height was 30 mm which 10 mm of the hollow fibers was incorporated in the scaffold (Figure 6).

PCL (Mw = 80kDa) was dissolved in solvent mixture of formic acid/ acetic acid (4/1) to obtain a 13% solution. The PCL solution delivered by the syringe pump at the flow rate of 1 mL/h to a 21-gauge blunt syringe needle which was horizontally fixed at 14 cm from the collector. High DC voltage was applied to the polymer solution at a voltage of +28 kV for needle. PCL porous hollow fibers were modified with sodium hydroxide 3 M for 30 min to create carboxyl and hydroxyl groups.

A mold for the correct placement of hollow fibers inside the scaffold was made by a 3D printer. PCL hollow fibers were placed at pre-defined locations in the mold and sugar crystals with size of 300–500 μm were added around the fibers in the mold. The mold containing fibers and sugar crystals was put in a humidified sealed container at 37°C for 16 hours to fuse the sugar crystals and left to dry at room temperature for 24 h. PLGA (75/25, PURAC Biomaterials, Netherlands) was dissolved in DMSO (Sigma) according to the concentration of 12.5% (w/v) and was thoroughly mixed with β-TCP particles (0.5–1 μm) (Nik Ceram Razi, Isfahan, Iran) according to the PLGA/β-TCP ratio of 2:1 (w/w). This mixture was then added dropwise to the mold allowing it to completely diffuse throughout the fused sugar crystals. Afterward, the mold was transferred to −20°C for 2 hours to set the mixture. Sugar crystals were leached out of the precipitated PLGA/β-TCP mixture in deionized water at room temperature for 3 days, during which time the water was changed approximately 3 times each day. The scaffolds were sterilized by 75% alcohol and washed 3 times with PBS followed by 30 min ultraviolet light.

Pre-treatment of hASCs with 1,25-$(OH)_2VitD_3$ and coculture of pre-treated hASCs and HUVECs

Human umbilical vein endothelial cells (HUVECs) were obtained from the National Cell Bank, Pasteur Institute of Iran (Tehran, Iran). Isolation procedure of human adipose stem cells (hASCs) was described by Overman et al.,[42] which heterogeneity studies, including cell characterization and multipotent differentiation potential of these cells, have been reported previously by their group[43,44] and proved that almost 90% of the hASCs within the freshly isolated SVF rapidly adhere to various scaffold types.[45]

hASCs were incubated for 30 minutes with/without 10^{-8} M 1,25-$(OH)_2VitD_3$ (Sigma-Aldrich) at room temperature. Then hASCs were washed with PBS, centrifuged, and re-suspended in Minimum Essential Medium Eagle Alpha Modification (α-MEM) without supplements. First, pre-treated hASCs which was seeded on PLGA/β-TCP/PCL scaffolds and cultured under static condition, compared with non-treated hASCs.

Secondly, HUVECs and hASCs were mixed in a proportion of 1:2.5 (10^6 HUVECs:2.5 × 10^6 hASCs)[19] and cultured in Dulbecco's Modified Eagle's Medium/Nutrient F-12 Ham (DMEM/F12) and α-MEM in same proportion.[26] Subsequently, 3.5 × 10^6 cells of the mixed cell suspension were added to each scaffold in a dropwise manner and incubated for 30 min. Thereafter, an additional 200 μl of culture medium was slowly added to each scaffold (three 30-minute cycles), after 2 hours, 10 ml of culture medium was added to each scaffold and hASCs/HUVECs-scaffolds were incubated in a humidified atmosphere at 37°C and 5% CO_2 overnight to allow cell attachment to the scaffolds. Scaffolds were also

cultured with 2.5×10^6 hASCs alone to be used as monoculture controls.

Dynamic culture using modified perfusion bioreactor versus static culture using flask bioreactor

After overnight static culture, a bioreactor group scaffolds, which were seeded by hASCs in a monoculture or 2.5:1 ratio with HUVECs (coculture group), were transferred to the modified perfusion bioreactors (one scaffold for each bioreactor), loaded with a total of 70 ml of culture medium (Figure 6). 30 ml of the culture medium was replaced twice a week for a total of two weeks. The static culture groups remained in the flask bioreactor with the same volume of culture medium. Cultures were divided into four groups: static coculture, dynamic coculture, static monoculture, dynamic monoculture.

A novel perfusion bioreactor system, developed in this study, was composed of the bioreactor as a main part containing a five-branch flow distributor which was connected to the PCL hollow fibers, tubing part, and a peristaltic pump (ISMATEC, Germany) with the flow rate of 3 ml/min. In case of nonexistence of culture medium in the main reservoir of bioreactor, the culture medium was flowed into the scaffold and it was observed that the culture medium was well distributed in the scaffold at 3 ml/min. At lower flow rates, the medium did not penetrate into the scaffold through PCL hollow fibers, and at higher flow rates, the PLGA/β-TCP scaffold degradation occurred too quickly within 14 days of culture. Inspired by previous studies mentioned in introduction section and our observations, the flow rate of 3 ml/min was selected.

hASCs/HUVECs proliferation on PLGA/β-TCP/PCL scaffolds

The alamarBlue® assay was used to assess cell viability. After overnight static culture and 14 days of dynamic culture, the hASCs/HUVECs-seeded scaffolds were treated in alamarBlue for 4 hours and fluorescence was read in medium samples at excitation 530 nm and emission 590 nm. We found a linear relationship between AlamarBlue fluorescence and cell number in both monoculture and coculture systems (data not shown).

Analysis of gene expression

Total RNA was extracted from hASCs cultured on PLGA/β-TCP/PCL scaffolds after 14 days, using TRIzol® reagent (Life Technologies™) according to the manufacturer's instruction, and stored at −80°C until further use. cDNA synthesis was performed in a thermocycler GeneAmp® PCR System9700 PE (Applied Biosystems, Foster City, CA, USA), using SuperScript® VILO™ cDNA Synthesis Kit (Life Technologies™) with 0.1 µg total RNA in a 20 µL reaction mix containing VILO™ Reaction Mix and SuperScript® Enzyme Mix. cDNA was stored at −20°C prior to real-time PCR analysis.

Real-time PCR reactions were performed using 1 µL of 5x diluted cDNA and SYBR® Green Mastermix (Roche Laboratories, IN, USA) according to the manufacturer's instructions in a LightCycler® (Roche Diagnostics). Real-time PCR conditions for all genes were as follows: 10 min pre-incubation at 95°C, followed by 45 cycles of amplification at 95°C for 2s, 56°C for 8s, 72°C for 10s, and 82°C for 5 s, after which melting curve analysis was performed. In each run the reaction mixture without cDNA was used as negative control. All primers used for real-time PCR were from Life Technologies™ (Supplementary Table S1). For quantitative real-time PCR, the values of relative gene expression were normalized using human 14-3-3 protein zeta/delta (YWHAZ) and hypoxanthine-guanine phosphoribosyltransferase (HPRT) housekeeping gene expression for Figure 1, and using beta2-microglobulin (B2m) housekeeping gene expression for Figure 5. Real-time PCR was used to assess expression of the following genes: alkaline phosphatase (ALP), osteopontin (OPN), osteonectin (SPARC), Runt-related transcription factor 2 (RUNX2), Osteocalcin

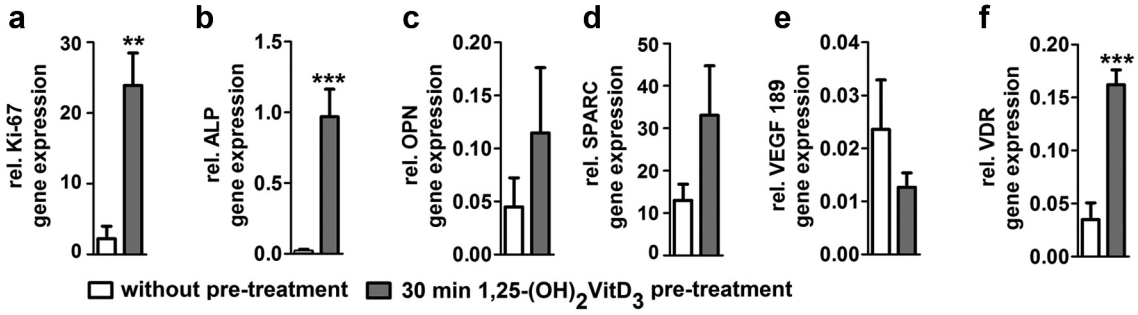

Figure 1. Short 1,25-$(OH)_2VitD_3$ pre-treatment effects on osteogenic and angiogenic gene expression of hASCs seeded on PLGA/β-TCP /PCL scaffold after 2 weeks. 30 min 1,25-$(OH)_2VitD_3$ pre-treatment increased (a) Ki-67 by 10.8-fold, (b) ALP by 43.2-fold, (c) OPN by 2.4-fold, (d) SPARC by 2.6-fold, decreased (e) $VEGF_{189}$ by 0.78-fold, and enhanced (f) VDR by 4.9-fold compared to non-treated controls. Values are mean ± SEM (n = 3). PLGA, poly(lactic-co-glycolic acid); β-TCP, β-tricalcium phosphate; PCL, Polycaprolactone, Ki-67, proliferation marker; ALP, alkaline phosphatase; OPN, osteopontin; SPARC, osteonectin; VEGF, vascular endothelial growth factor; VDR, vitamin D nuclear receptor. Significantly different from control, **p < .01, ***p < .001.

(OCN), cytochrome P450 family 27 subfamily B member 1 (CYP27B1), vitamin D receptor (VDR), vascular endothelial growth factor ($VEGF_{165}$ and $VEGF_{189}$), Endothelin 1 (ET-1), and proliferation marker (ki-67). In each assay for osteogenic markers, cDNA from osteoblasts or human reference (Agilent Technologies, Stratagene Products Division, La Jolla, CA, USA) was used as reference DNA. With Light Cycler® software (version 1.2), crossing points were assessed and plotted versus the serial dilution of known concentrations of the reference DNA (2.5–0.004 ng/µL). Gene expression was compared between cells seeded on 3D scaffolds in monoculture or coculture conditions under static or dynamic cultivation.

ALP activity assay and protein assay

ALP activity was measured to assess the osteoblastic phenotype of hASC seeded on BCP20/80 scaffolds. After 14 days of culture, the scaffolds were transferred to 24-well culture plates (Cellstar, Frickenhausen, Germany) and washed with PBS. The cells were lysed with cOmplete™ Lysis-M buffer to determine ALP activity and protein content. *P*-nitrophenyl-phosphate (Fluka, Poole, UK) at pH 10.3 was used as substrate for ALP. The absorbance was read at 405 nm using a ELISA reader (Stat Fax 2100, Awareness Technology Inc., USA). ALP activity was expressed as µmoles of *p*-nitrophenol formed per hour per milligram of cellular protein. After 14 days of culture, ALP activity was also visualized using nitro blue tetrazolium chloride/5-bromo-4-chloro-3-indolyl phosphate (NBT/BCIP; Roche, Mannheim, Germany) following the standard protocol. The amount of protein was determined by using a BCA Protein Assay reagent Kit (Pierce™, Rockford, III, USA), and the absorbance was read at 540 nm with a ELISA reader (Stat Fax 2100, Awareness Technology Inc., USA).

Scanning electron microscopy (SEM)

SEM was used to study micro-surrounding of the cells on the scaffold. To carry out a SEM analysis, the cells in the scaffolds were fixed in 2.5% glutaraldehyde, overnight. After washing with PBS, the cultured scaffolds were dehydrated serially in ethanol 30, 50, 70, 80, 90, and 100% and then dried with CO_2 critical point dryer and coated with gold. The samples were imaged by SEM (AIS2100, Seron Technologies, South Korea).

Statistical analysis

Data obtained using hASCs were expressed as mean ± SEM. The effect of 1,25-$(OH)_2VitD_3$ treatment compared to non-treated cells and the effect of dynamic mono/coculture compared to static mono/coculture was tested with the Student's t-test for single group mean. ANOVA two-way analysis of variance was used to compare attachment data between treated cells and non-treated

cells as well as static and dynamic culture. Differences were considered significant if $p < .05$. Statistical analysis was performed using GraphPad Prism® 5.01 (GraphPad Software Inc., La Jolla, CA, USA). All experiments were performed in triplicate.

RESULTS

Effect of 30 min pre-treatment with 1,25-$(OH)_2$VitD$_3$ on osteogenic gene expression of hASCs

30 min 1,25-$(OH)_2$VitD$_3$ pre-treatment increased proliferation marker (ki-67) by 10.8-fold, ALP by 43.2-fold, osteopontin (OPN) by 2.4-fold, osteonectin (SPARC) by 2.6-fold, decreased $VEGF_{189}$ by 0.78-fold, and enhanced vitamin D receptor (VDR) expression by 4.9-fold in hASCs seeded on PLGA/β-TCP/PCL scaffold after 14 days of static monoculture, compared to non-treated controls (Figure 1) which also agrees with our previous reported data.[41] We reported a similar results regarding hASCs seeded on biphasic calcium phosphate scaffold composed of 20% hydroxyapatite and 80% β-TCP in which the highest ALP activity occurred on day 14.[41] Based on our previous data, the number of days for static and dynamic culture in this study was selected 14 days.

Effect of hASC–HUVEC coculture on cell proliferation

Static coculture, dynamic coculture, static monoculture, and dynamic monoculture increased proliferation by 2.79-fold, 2.91-fold, 2.98-fold, and 3.11-fold, respectively, after 14 days, without any significant difference between the comparing groups (Figure 2a).

Effect of dynamic hASC–HUVEC coculture and hASC monoculture on ALP activity

ALP activity of hASCs after 14 days of dynamic coculture was increased by 7.1-fold compared to static coculture, while ALP activity of dynamic monoculture was increased 24.1-fold relative to static monoculture after 2 weeks of culture (Figure 2b). ALP activity of static coculture was increased by 2.2-fold relative to static monoculture. Dynamic monoculture increased ALP activity by

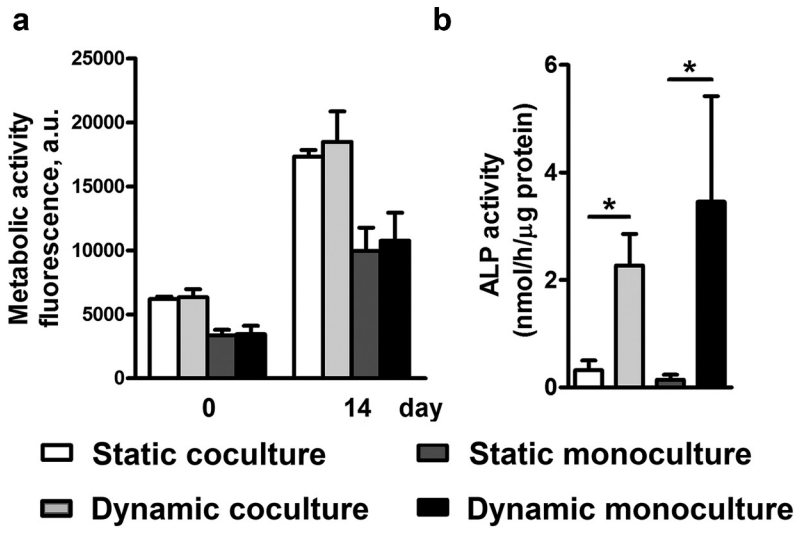

Figure 2. Dynamic co/monoculture versus static co/monoculture effects on metabolic activity and ALP activity of hASCs. hASCs were pre-treated for 30 min with 1,25-$(OH)_2$VitD$_3$ and cocultured with HUVECs in a modified perfusion bioreactor (dynamic culture) and flask bioreactor (static culture) for 14 days. (a) Static coculture, dynamic coculture, static monoculture and dynamic monoculture increased proliferation by 2.79-fold, 2.91-fold, 2.98-fold, and 3.11-fold, respectively. (b) Dynamic coculture increased ALP activity by 7.1-fold compared to static coculture and dynamic monoculture increased ALP activity by 24.1-fold compared to static monoculture. Values are mean ± SEM (n = 3). ALP, alkaline phosphatase; hASCs, human adipose stem cells; 1,25-$(OH)_2$VitD$_3$, 1,25-dihydroxyvitamin D$_3$. HUVEC, human umbilical vein endothelial cells. *Significantly different from static culture, $p < .05$.

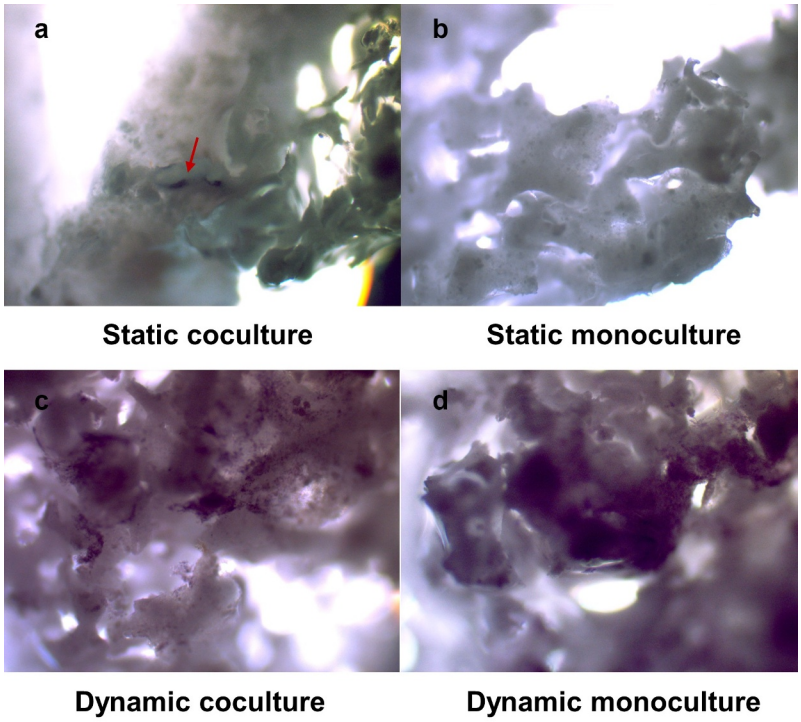

Figure 3. hASCs were stained for ALP activity using NBT/BCIP. hASCs were pre-treated for 30 min with 1,25-$(OH)_2VitD_3$ and cocultured with HUVECs in static and dynamic culture for 14 days. Dynamic co/monoculture notably increased ALP activity compared to the static co/monoculture. hASCs, human adipose stem cells; ALP, alkaline phosphatase; NBT/BCIP, nitro blue tetrazolium chloride/5-bromo-4-chloro-3-indolyl phosphate; HUVEC, human umbilical vein endothelial cells, 40X magnification.

1.5-fold, compared with dynamic coculture. Moreover, this was also confirmed by ALP staining after 14 days of culture to better visualize the ALP activity (Figure 3). The cells were also observed using scanning electron microscopy (SEM) to confirm the micro-surrounding of the cells on the scaffold (Figure 4).

Effect of hASC–HUVEC coculture and hASC monoculture on osteogenic and angiogenic differentiation

Osteogenic and angiogenic gene markers were quantified for all samples of static coculture, dynamic coculture, static monoculture, and dynamic monoculture system (Figure 5). Osteogenic gene markers included runt-related transcription factor 2 (RUNX2) as a well-known master transcriptional regulators of skeletogenesis,[46] OPN as a crucial marker for bone remodeling and biomineralization,[47] SPARC which regulates the activity of osteoblasts and osteoclasts and is expressed by osteoblasts undergoing active matrix deposition,[48] and osteocalcin (OCN) which mediates biomineralization during osteogenic maturation,[11] were analyzed. Angiogenic gene markers including Endothelin-1 which is implicated in the signaling between vascular endothelial cells and osteoblasts during bone development, remodeling and repair,[49] and VEGF which contributes to coupling of osteogenesis to angiogenesis and bone healing during different phases of bone repair[50] were also analyzed. $VEGF_{189}$ contains two heparin-binding sites and therefore sequestered in the ECM, and $VEGF_{165}$ is the most abundant isoform containing one heparin binding site.[50]

Analyzed gene expression showed that (i) static coculture increased Ki-67 expression by 72-fold, RUNX2 by 12-fold, OPN by 2.8-fold, SPARC by 4.2-fold, OCN by 2.9-fold, $VEGF_{165}$ by 5.8-fold, $VEGF_{189}$ by 9-fold, Endothelin-1 by 154-fold, and

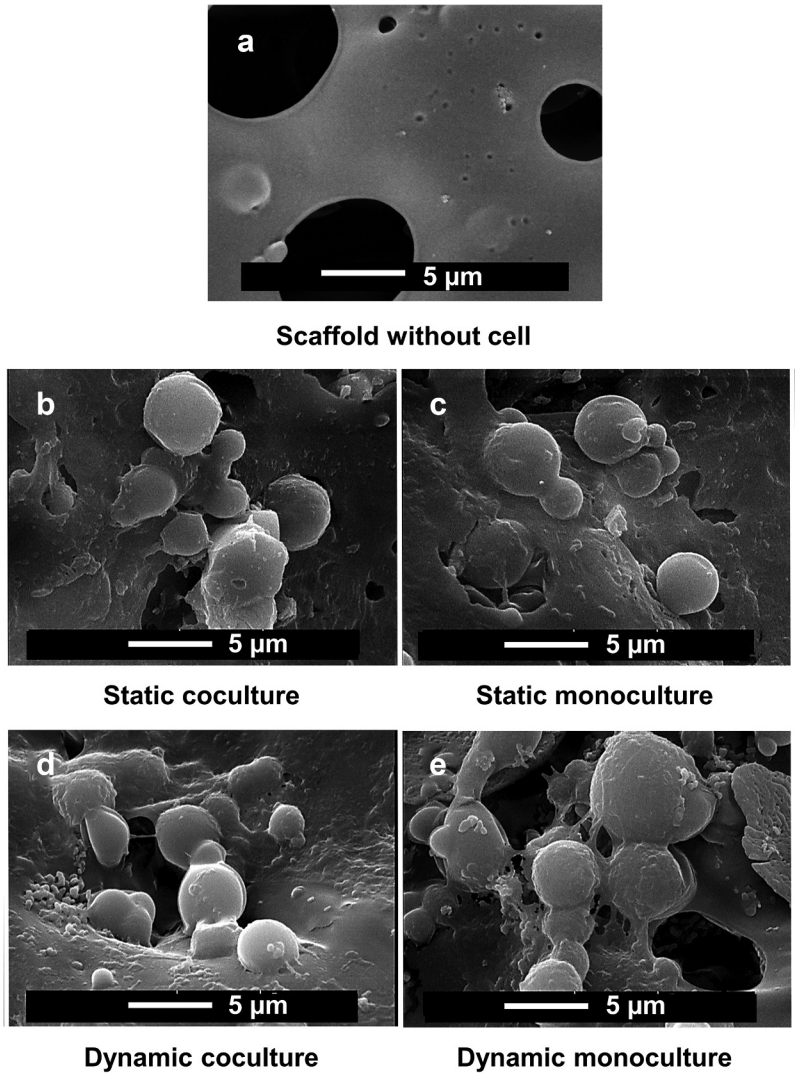

Figure 4. The cells was visualized using scanning electron microscopy (SEM) to confirm the micro-surrounding of the cells on PLGA/β-TCP/PCL scaffold. hASCs were pre-treated for 30 min with 1,25-$(OH)_2VitD_3$ and cocultured with HUVECs in static and dynamic culture for 14 days. PLGA, poly(lactic-co-glycolic acid); β-TCP, β-Tricalcium phosphate; PCL, Polycaprolactone; hASCs, human adipose stem cells; 25-$(OH)_2VitD_3$, 1,25-dihydroxyvitamin D_3; HUVEC, human umbilical vein endothelial cells.

CYP27B1 by 7-fold, compared to static monoculture.

(ii) Dynamic coculture increased Ki-67 expression by 6.8-fold, $VEGF_{165}$ by 6-fold, $VEGF_{189}$ by 2-fold, Endothelin-1 by 4-fold, and CYP27B1 by 5-fold, compared to dynamic monoculture. Although, dynamic monoculture increased RUNX2 expression by 1.8-fold, OPN by 1.4-fold, SPARC by 2.9-fold, and OCN by 1.4-fold, compared to dynamic coculture.

(iii) Dynamic monoculture increased Ki-67 expression by 5-fold, RUNX2 by 10.9-fold, OPN by 8.6-fold, SPARC by 10.4-fold, OCN by 4-fold, $VEGF_{165}$ by 1.1-fold, $VEGF_{189}$ by 5.7-fold, Endothelin-1 by 35-fold, and CYP27B1 by 15.4-fold, compared to static monoculture.

(iv) Dynamic coculture increased $VEGF_{165}$ expression by 1.2-fold, $VEGF_{189}$ by 1.3-fold, OPN by 2.1-fold, and decreased RUNX2 by 0.5-fold and Ki-67 by 0.5-fold compared to static coculture, although SPARC, OCN, and Endothelin1 genes were almost equally expressed in both static and dynamic coculture.

DISCUSSION

Here we investigated whether flow perfusion culture would affect osteogenic and angiogenic

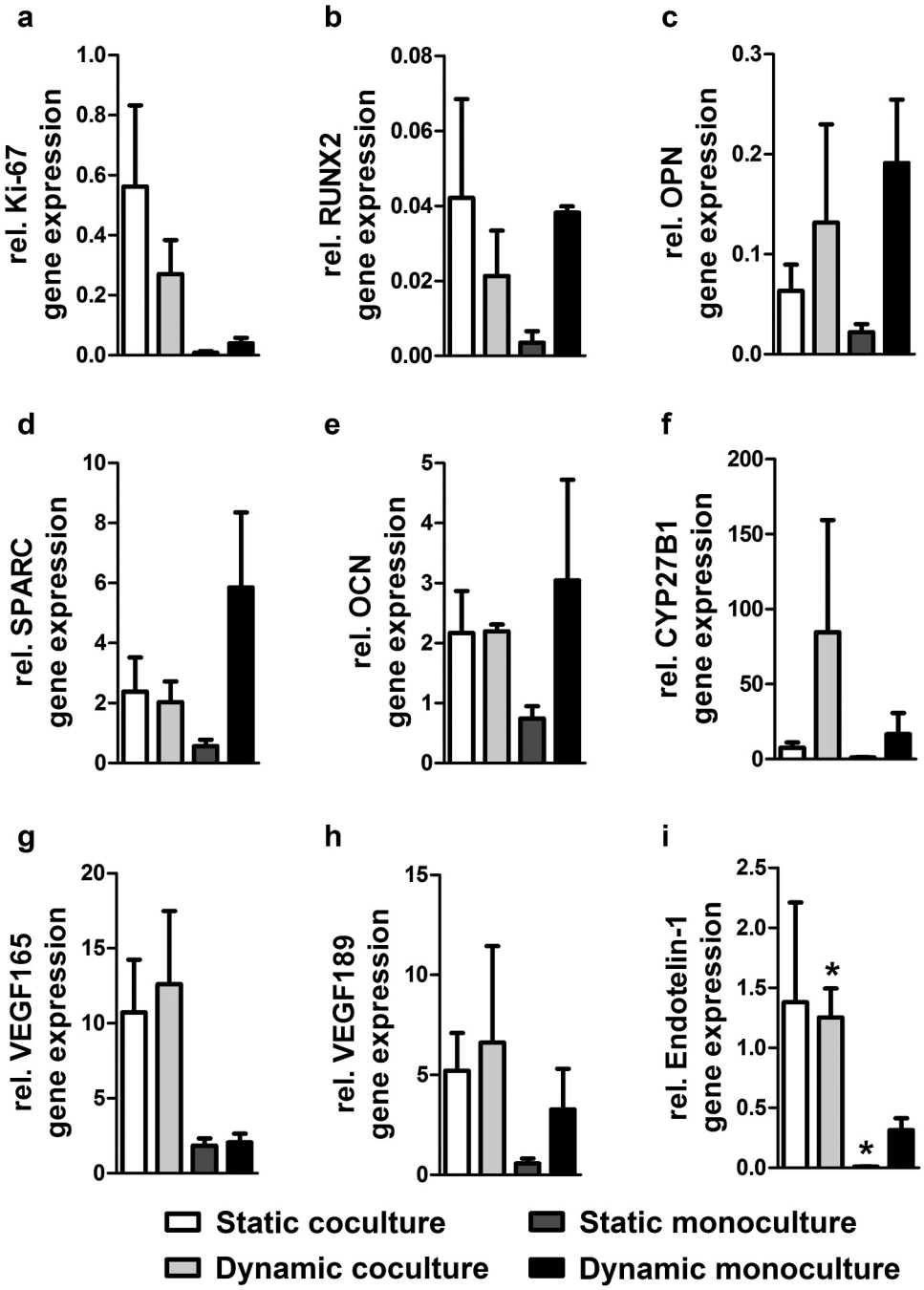

Figure 5. Dynamic co/monoculture versus static co/monoculture effects on osteogenic gene expression of hASCs and angiogenic gene expression of the accumulation of cells on PLGA/β-TCP/PCL scaffold. Pre-treated hASCs with 1,25-$(OH)_2VitD_3$ cocultured with HUVECs in static and dynamic culture for 14 days. Dynamic coculture increased (a) Ki-67 expression by 6.8-fold; decreased (b) RUNX2 by 0.55-fold, (c) OPN by 0.71-fold, (d) SPARC by 0.33-fold, and (e) OCN by 0.71-fold; increased (f) CYP27B1 by 5-fold (g) $VEGF_{165}$ by 6-fold, (h) $VEGF_{189}$ by 2-fold, and (i) Endothelin-1 by 4-fold compared to dynamic monoculture. Values are mean ± SEM (n = 3). PLGA, poly(lactic-co-glycolic acid); β-TCP, β-Tricalcium phosphate; PCL, Polycaprolactone; Ki-67, proliferation marker; RUNX2, Runt-related transcription factor 2; OPN, osteopontin; SPARC, osteonectin; OCN, osteocalcin; CYP27B1, cytochrome P450 family 27 subfamily B member 1; VEGF, vascular endothelial growth factor. *Significantly different from dynamic monoculture, $p < .05$.

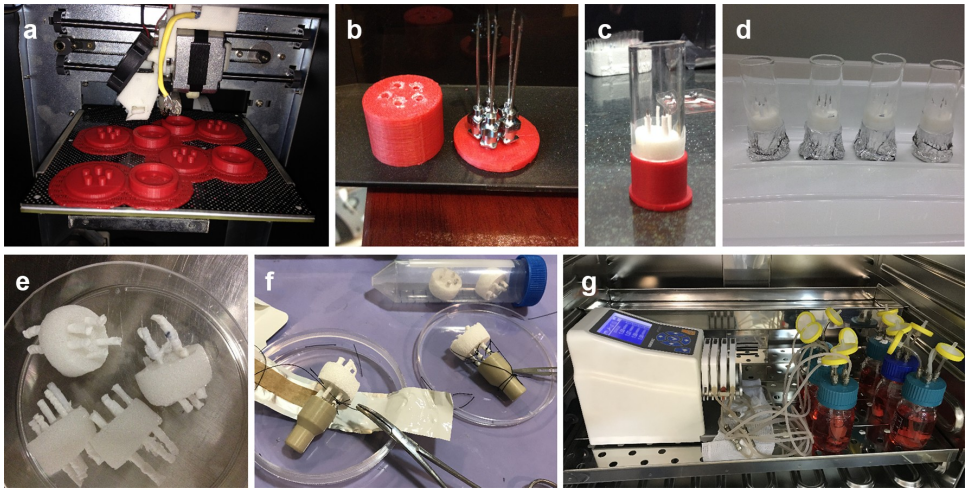

Figure 6. Design and preparation of (a) 3D printed mold for the correct placement of hollow fibers inside the scaffold; (b) pre-defined locations of hollow fibers in the mold; (c,d) cylindrical glass for adding sugar crystals around the fibers; (e) PLGA/β-TCP/PCL scaffold. (f) Connecting five-branch distributor to the scaffold. (g) Modified perfusion bioreactor system.

differentiation of coculture of HUVECs and hASCs, and compared with static and dynamic monoculture of hASCs. The ultimate goal was to promote osteogenic and angiogenic synergy of hASCs and HUVECs in large bone tissue-engineered constructs (thickness≥1 cm) for the reconstruction of critical-sized bone defects; although animal studies is required to fulfill this goal and realize the implication of this technique *in vivo*.

We found that (i) 30 min 1,25-$(OH)_2VitD_3$ pre-treatment of hASCs enhanced expression of proliferative and osteogenic differentiation markers more than non-treated controls, (ii) in case of static culture, osteogenic and angiogenic gene expression of hASC–HUVEC coculture systems was more pronounced than that by hASC monoculture, (iii) in case of dynamic culture, although hASC monoculture increased osteogenic gene expression more than hASC–HUVEC coculture, angiogenic markers in hASC–HUVEC coculture was more significantly expressed at day 14, compared to monoculture, (iv) dynamic monoculture notably increased osteogenic and angiogenic gene expression compared to static monoculture, (v) dynamic coculture enhanced $VEGF_{165}$, $VEGF_{189}$, and OPN gene expression and ALP activity compared to static coculture. Although SPARC, OCN, and Endothelin1 genes almost equally expressed in both static and dynamic coculture system. RUNX2 and Ki-67 gene expression of dynamic coculture was lower than static coculture. (vi) no significant differences in proliferation was observed between the groups.

We found that $VEGF_{189}$, $VEGF_{165}$, and Endothelin-1 genes in coculture group expressed at a higher value than in monoculture which signifies the heightened angiogenic potential of coculture group,[51–53] which is in line with recent findings of Chen et al. using coculture of human BMSCs and HUVEC,[16] Cai et al. using hASCs and HUVEC,[26] Kook et al. using hASCs and HUVEC,[25] and Liang et al. using coculture of human BMSCs and endothelial progenitor cells under static culture.[27] A comparable result has been also reported that direct co-culture of endothelial progenitor cells and BMSCs under static culture enhances vascularization and osteogenesis due to cell–cell communication both *in vitro* and *in vivo*.[54] Lastly, it has been revealed a significant increase of VEGF expression in static ASC-EC co-culture compared to static BMSC-EC co-culture.[55]

Flowing blood creates a frictional force called shear stress that has noticeable effects on vascular function by activating mechanosensitive signaling pathways in vascular endothelial cells.[56] Laminar shear stress can directly activate growth factor receptors on stem/progenitor cells, initiating signaling pathways leading toward endothelial cell differentiation.[57] The shear stress created by

dynamic culture contributes to hASCs differentiation into endothelial-like cells.[58] Dynamic coculture contributes to the improvement of angiogenic marker expression ($VEGF_{165}$ and $VEGF_{189}$) compared to static coculture at day 14, as also reported by Nguyen et al. using coculture of human BMSCs and HUVEC in tubular perfusion system.[32] On the basis of similar finding with BMSCs, dynamic loading directs stem cell behavior toward VEGF gene expression.[59] As observed in an earlier study, dynamic co-culture of HUVECs and human smooth muscle cells within a perfusion bioreactor generates early microvascular network in natural and synthetic bone scaffolds through EC lumen formation within decellularized native bone and upregulating EC-specific gene expression of HUVECs cultured on 3D-printed hyperelastic bone scaffolds.[60]

According to our findings, dynamic coculture decreased expression of early osteogenic marker (RUNX2) and increased expression of intermediate osteogenic marker (OPN) and significantly enhanced ALP activity compared to static coculture which signifies the start of new bone formation and mineralization by hASCs. No differences were observed in expression of late osteogenic markers (SPARC and OCN) between static and dynamic cocultures. These changes in the osteogenic behavior and dynamic gene expression patterns support the idea of combining both static and dynamic environments into a coculture system.[32]

All in all, static coculture significantly enhanced osteogenic and angiogenic differentiation at day 14 compared to static monoculture. Due to significant increase in ALP activity and enhanced expression of angiogenic markers, dynamic coculture is in preference to static coculture. Dynamic coculture has high priority compared with dynamic monoculture due to enhanced expression of angiogenic markers. Other studies have revealed other aspects of dynamic culture and reported that dynamic mechanical stimuli during the culture period improve the mechanical properties of the tissue-engineered vessels by more collagen and elastin expression within the extracellular matrix (ECM).[61] In addition, fluid shear stress has a positive effect on the biomineralization process of tissue-engineered bone, as evidenced by the enhanced degree of collagen self-assembly and the accelerated speed of amorphous calcium phosphate formation and transition.[62]

The role of CYP27B1 is in vitamin D hormone activation by converting 25-hydroxyvitamin D to $1,25\text{-}(OH)_2D_3$. Hence, the presence of $1,25\text{-}(OH)_2D_3$ inhibit CYP27B1 gene expression.[40] Upregulation of CYP27B1 expression in dynamic coculture may lead to inhibition of $1,25\text{-}(OH)_2VitD_3$ activity which subsequently downregulated osteogenesis. In contrast to dynamic hASCs monocultures, dynamic cocultures showed less osteogenic gene expression and related protein content, but much more angiogenic gene expression. Indeed, in dynamic coculture system, osteogenic and angiogenic differentiation have synchronous synergy, which is a prerequisite for the performance and life span of tissue-engineered bone implant *in vivo*.

Flow perfusion in dynamic monoculture of hASCs significantly upregulated ALP activity and expression of osteogenic genes compared with static monoculture which agrees with findings by others using ASCs[63] and BMSCs.[64] Moreover, we found that dynamic monoculture enhanced angiogenic gene expression of hASCs compared to static monoculture. Increased angiogenesis in dynamically cultivated MSC aggregates may be promising for future clinical application.[8]

In conclusion, we used ALP assay, ALP staining, AlamarBlue assay, analysis of osteogenic and angiogenic gene expression to evaluate the synergistic effects of flow perfusion and cocultured hASCs with HUVECs on osteogenesis and angiogenesis of the accumulation of cells. As compared to monocultures, flow perfusion and coculture condition synergistically enhanced angiogenic gene expression of the accumulation of cells. In dynamic culture, although hASC monoculture increased osteogenic gene expression more than hASC–HUVEC coculture, angiogenic markers in hASC–HUVEC coculture was more significantly expressed compared to monoculture. In static culture, osteogenic and angiogenic gene expression of hASC–HUVEC coculture systems was more pronounced than that by monoculture. Altogether, dynamic culture has considerable advantage over static culture in terms of ALP activity. Dynamic cocultures

of hASCs and HUVECs enhanced synergistic effect of angiogenic and osteogenic differentiation more strongly than dynamic monoculture of hASCs, suggesting that it represents a promising approach for bone tissue regeneration. Although, the further step entails animal studies to prove the applicability of the current technique *in vivo*.

Acknowledgments

The work of F. Mokhtari-Jafari was financially sponsored by a grant from the University of Tehran for the stimulation of academically talented students in Iran. We would like to thank Behrouz Zandieh-Doulabi from Academic Centre for Dentistry Amsterdam (ACTA) - Vrije Universiteit Amsterdam for his help to perform real-time PCR.

Disclosure statement

The authors declare no conflicts of interest.

ORCID

Fatemeh Mokhtari-Jafari http://orcid.org/0000-0003-4367-6468
Massoumeh Jabbari Fakhr http://orcid.org/0000-0001-7279-2447
Yasaman Zamani http://orcid.org/0000-0002-3687-2471

References

1. Bao X, Zhu L, Huang X, Tang D, He D, Shi J, Xu G. 3D biomimetic artificial bone scaffolds with dual-cytokines spatiotemporal delivery for large weight-bearing bone defect repair. Sci Rep. 2017;7(1):7814. doi:10.1038/s41598-017-08412-0. PMID: 28798376.
2. Zhang H, Mao X, Zhao D, Jiang W, Du Z, Li Q, Jiang C, Han D. Three dimensional printed polylactic acid-hydroxyapatite composite scaffolds for prefabricating vascularized tissue engineered bone: an in vivo bioreactor model. Sci Rep. 2017;7(1):15255. doi:10.1038/s41598-017-14923-7.
3. Zhu M, Li W, Dong X, Yuan X, Midgley AC, Chang H, Wang Y, Wang H, Wang K, Ma PX. In vivo engineered extracellular matrix scaffolds with instructive niches for oriented tissue regeneration. Nat Commun. 2019;10(1):4620. doi:10.1038/s41467-019-12545-3.
4. Salamon D, Teixeira S, Dutczak SM, Stamatialis DF. Facile method of building hydroxyapatite 3D scaffolds assembled from porous hollow fibers enabling nutrient delivery. Ceram Int. 2014;40(9):14793–99. doi:10.1016/j.ceramint.2014.06.071.
5. Barry M, Pearce H, Cross L, Tatullo M, Gaharwar AK. Advances in nanotechnology for the treatment of osteoporosis. Curr Osteoporos Rep. 2016;14(3):87–94. doi:10.1007/s11914-016-0306-3.
6. Marrelli M, Maletta C, Inchingolo F, Alfano M, Tatullo M. Three-point bending tests of zirconia core/veneer ceramics for dental restorations. Int J Dent. 2013;2013:831976. doi:10.1155/2013/831976.
7. Ballini A, Cantore S, Scacco S, Coletti D, Tatullo M. Mesenchymal stem cells as promoters, enhancers, and playmakers of the translational regenerative medicine 2018. Stem Cells Int. 2018;2018:6927401. doi:10.1155/2018/6927401.
8. Egger D, Tripisciano C, Weber V, Dominici M, Kasper C. Dynamic cultivation of mesenchymal stem cell aggregates. Bioengineering (Basel). 2018;5(2):48. doi:10.3390/bioengineering5020048.
9. Tatullo M, Codispoti B, Pacifici A, Palmieri F, Marrelli M, Pacifici L, Paduano F. Potential use of human periapical cyst-mesenchymal stem cells (hPCy-MSCs) as a novel stem cell source for regenerative medicine applications. Front Cell Dev Biol. 2017;5:103. doi:10.3389/fcell.2017.00103.
10. Pizzicannella J, Diomede F, Merciaro I, Caputi S, Tartaro A, Guarnieri S, Trubiani O. Endothelial committed oral stem cells as modelling in the relationship between periodontal and cardiovascular disease. J Cell Physiol. 2018;233(10):6734–47. doi:10.1002/jcp.26515.
11. Tsao YT, Huang YJ, Wu HH, Liu YA, Liu YS, Lee OK. Osteocalcin mediates biomineralization during osteogenic maturation in human mesenchymal stromal cells. Int J Mol Sci. 2017;18(1):159. doi:10.3390/ijms18010159.
12. Farre-Guasch E, Bravenboer N, Helder MN, Schulten E, Ten Bruggenkate CM, Klein-Nulend J. Blood vessel formation and bone regeneration potential of the stromal vascular fraction seeded on a calcium phosphate scaffold in the human maxillary sinus floor elevation model. Materials (Basel). 2018;11(1):161. doi:10.3390/ma11010161.
13. Lu H, Wang F, Mei H, Wang S, Cheng L. Human adipose mesenchymal stem cells show more efficient angiogenesis promotion on endothelial colony-forming cells than umbilical cord and endometrium. Stem Cells Int. 2018;2018:7537589. doi:10.1155/2018/7537589.
14. Panina YA, Yakimov AS, Komleva YK, Morgun AV, Lopatina OL, Malinovskaya NA, Shuvaev AN, Salmin VV, Taranushenko TE, Salmina AB. Plasticity of adipose tissue-derived stem cells and regulation of angiogenesis. Front Physiol. 2018;9:1656. doi:10.3389/fphys.2018.01656.
15. Probst FA, Fliefel R, Burian E, Probst M, Eddicks M, Cornelsen M, Riedl C, Seitz H, Aszódi A, Schieker M. Bone regeneration of minipig mandibular defect by adipose derived mesenchymal stem cells seeded tri-calcium phosphate- poly(D,L-lactide-co-glycolide) scaffolds. Sci Rep. 2020;10(1):2062. doi:10.1038/s41598-020-59038-8.

16. Chen J, Deng L, Porter C, Alexander G, Patel D, Vines J. Angiogenic and osteogenic synergy of human mesenchymal stem cells and human umbilical vein endothelial cells cocultured on a nanomatrix. Sci Rep. 2018;8(1):15749. doi:10.1038/s41598-018-34033-2.
17. Chen W, Liu X, Chen Q, Bao C, Zhao L, Zhu Z, Xu HHK. Angiogenic and osteogenic regeneration in rats via calcium phosphate scaffold and endothelial cell coculture with hBMSCs, hUCMSCs, hiPSC-MSCs and hESC-MSCs. J Tissue Eng Regen Med. 2018;12(1):191–203. doi:10.1002/term.2395.
18. Bretschneider H, Quade M, Lode A, Gelinsky M, Rammelt S, Zwingenberger S, Schaser KD, Vater C. Characterization of naturally occurring bioactive factor mixtures for bone regeneration. Int J Mol Sci. 2020;21(4):1412. doi:10.3390/ijms21041412.
19. Roux BM, Akar B, Zhou W, Stojkova K, Barrera B, Brankov JG. Preformed vascular networks survive and enhance vascularization in critical sized cranial defects. Tissue Eng Part A. 2018;24(21–22):1603–15. doi:10.1089/ten.tea.2017.0493.
20. Shah AR, Wenke JC, Agrawal CM. Manipulation of human primary endothelial cell and osteoblast coculture ratios to augment vasculogenesis and mineralization. Ann Plas Surg. 2016;77(1):122–28. doi:10.1097/SAP.0000000000000318.
21. De Moor L, Merovci I, Baetens S, Verstraeten J, Kowalska P, Krysko DV, Vos WHD, Declercq H. High-throughput fabrication of vascularized spheroids for bioprinting. Biofabrication. 2018;10(3):035009. doi:10.1088/1758-5090/aac7e6.
22. Inglis S, Kanczler JM, Oreffo ROC. 3D human bone marrow stromal and endothelial cell spheres promote bone healing in an osteogenic niche. Faseb J. 2019;33(3):3279–90. doi:10.1096/fj.201801114R.
23. Freitas GP, Lopes HB, Souza ATP, Oliveira PGFP, Almeida ALG, Souza LEB, Coelho PG, Beloti MM, Rosa AL. Cell therapy: effect of locally injected mesenchymal stromal cells derived from bone marrow or adipose tissue on bone regeneration of rat calvarial defects. Sci Rep. 2019;9(1):13476. doi:10.1038/s41598-019-50067-6.
24. Mazini L, Rochette L, Amine M, Malka G. Regenerative capacity of adipose derived stem cells (ADSCs), comparison with mesenchymal stem cells (MSCs). Int J Mol Sci. 2019;20(10):2523. doi:10.3390/ijms20102523.
25. Kook YM, Kim H, Kim S, Heo CY, Park MH, Lee K, Heo CY, Park MH, Koh WG. Promotion of vascular morphogenesis of endothelial cells co-cultured with human adipose-derived mesenchymal stem cells using polycaprolactone/gelatin nanofibrous scaffolds. Nanomaterials (Basel). 2018;8:117. doi:10.3390/nano8020117.
26. Cai X, Xie J, Yao Y, Cun X, Lin S, Tian T, Zhu B, Lin Y. Angiogenesis in a 3D model containing adipose tissue stem cells and endothelial cells is mediated by canonical wnt signaling. Bone Res. 2017;5:17048. doi:10.1038/boneres.2017.48.
27. Liang T, Zhu L, Gao W, Gong M, Ren J, Yao H, Wang K, Shi D. Coculture of endothelial progenitor cells and mesenchymal stem cells enhanced their proliferation and angiogenesis through PDGF and notch signaling. FEBS Open Bio. 2017;7(11):1722–36. doi:10.1002/2211-5463.12317.
28. Li Y, Liu Z, Tang Y, Feng W, Zhao C, Liao J, Zhang C, Chen H, Ren Y, Dong S. Schnurri-3 regulates BMP9-induced osteogenic differentiation and angiogenesis of human amniotic mesenchymal stem cells through Runx2 and VEGF. Cell Death Dis. 2020;11(1):72. doi:10.1038/s41419-020-2279-5.
29. Jia Y, Zhu Y, Qiu S, Xu J, Chai Y. Exosomes secreted by endothelial progenitor cells accelerate bone regeneration during distraction osteogenesis by stimulating angiogenesis. Stem Cell Res Ther. 2019;10(1):12. doi:10.1186/s13287-018-1115-7.
30. Tsimbouri PM, Childs PG, Pemberton GD, Yang J, Jayawarna V, Orapiriyakul W, Burgess K, González-García C, Blackburn G, Thomas D. Stimulation of 3D osteogenesis by mesenchymal stem cells using a nanovibrational bioreactor. Nat Biomed Eng. 2017;1(9):758–70. doi:10.1038/s41551-017-0127-4.
31. Harvestine JN, Gonzalez-Fernandez T, Sebastian A, Hum NR, Genetos DC, Loots GG, Leach JK. Osteogenic preconditioning in perfusion bioreactors improves vascularization and bone formation by human bone marrow aspirates. Sci Adv. 2020;6(7):eaay2387. doi:10.1126/sciadv.aay2387.
32. Nguyen BB, Moriarty RA, Kamalitdinov T, Etheridge JM, Fisher JP. Collagen hydrogel scaffold promotes mesenchymal stem cell and endothelial cell coculture for bone tissue engineering. J Biomed Mater Res A. 2017;105:1123–31. doi:10.1002/jbm.a.36008.
33. Lovecchio J, Gargiulo P, Vargas Luna JL, Giordano E, Sigurjónsson ÓE. A standalone bioreactor system to deliver compressive load under perfusion flow to hBMSC-seeded 3D chitosan-graphene templates. Sci Rep. 2019;9(1):16854. doi:10.1038/s41598-019-53319-7.
34. Weyand B, Kasper C, Israelowitz M, Gille C, von Schroeder HP, Reimers K, Vogt PM. A differential pressure laminar flow reactor supports osteogenic differentiation and extracellular matrix formation from adipose mesenchymal stem cells in a macroporous ceramic scaffold. Biores Open Access. 2012;1(3):145–56. doi:10.1089/biores.2012.9901.
35. Kim KM, Choi YJ, Hwang JH, Kim AR, Cho HJ, Hwang ES, Park JY, Lee SH, Hong JH. Shear stress induced by an interstitial level of slow flow increases the osteogenic differentiation of mesenchymal stem cells through TAZ activation. PloS One. 2014;9(3):e92427. doi:10.1371/journal.pone.0092427.
36. Yeatts AB, Fisher JP. Tubular perfusion system for the long-term dynamic culture of human mesenchymal stem cells. Tissue Eng Part C Methods. 2011;17(3):337–48. doi:10.1089/ten.tec.2010.0172.

37. Yang Y, Zhao Y, Tang G, Li H, Yuan X, Fan Y. In vitro degradation of porous poly(l-lactide-co-glycolide)/β-tricalcium phosphate (PLGA/β-TCP) scaffolds under dynamic and static conditions. Polym Degrad Stab. 2008;93(10):1838–45. doi:10.1016/j.polymdegradstab.2008.07.007.
38. Zhang Y, Yang W, Devit A, Van Den Beucken JJJP. Efficiency of coculture with angiogenic cells or physiological BMP-2 administration on improving osteogenic differentiation and bone formation of MSCs. J Biomed Mater Res A. 2019;107(3):643–53. doi:10.1002/jbm.a.36581.
39. Marrazzo P, Paduano F, Palmieri F, Marrelli M, Tatullo M. Highly efficient in vitro reparative behaviour of dental pulp stem cells cultured with standardised platelet lysate supplementation. Stem Cells Int. 2016;2016:7230987. doi:10.1155/2016/7230987.
40. Lou YR, Toh TC, Tee YH, Yu H. 25-Hydroxyvitamin D3 induces osteogenic differentiation of human mesenchymal stem cells. Sci Rep. 2017;7(1):42816. doi:10.1038/srep42816.
41. Mokhtari-Jafari F, Amoabediny G, Mm D, Mn H, Zandieh-Doulabi B, Klein-Nulend J. Short pretreatment with calcitriol is far superior to continuous treatment in stimulating proliferation and osteogenic differentiation of human adipose stem cells. Cell J. 2020;22:293–301. doi:10.22074/cellj.2020.6773.
42. Overman JR, Farre-Guasch E, Helder MN, ten Bruggenkate CM, Schulten EA, Klein-Nulend J. Short (15 minutes) bone morphogenetic Protein-2 treatment stimulates osteogenic differentiation of human adipose stem cells seeded on Calcium Phosphate scaffolds in vitro. Tissue Eng Part A. 2013;19(3–4):571–81. doi:10.1089/ten.tea.2012.0133.
43. Varma MJO, Breuls RGM, Schouten TE, Jurgens WJFM, Bontkes HJ, Schuurhuis GJ, Van Ham SM, van Milligen FJ. Phenotypical and functional characterization of freshly isolated adipose tissue-derived stem cells. Stem Cells Dev. 2007;16(1):91–104. doi:10.1089/scd.2006.0026.
44. Jurgens WJFM, van Dijk A, Doulabi BZ, Niessen FB, Ritt MJPF, van Milligen FJ, Helder MN. Freshly isolated stromal cells from the infrapatellar fat pad are suitable for a one-step surgical procedure to regenerate cartilage tissue. Cytotherapy. 2009;11(8):1052–64. doi:10.3109/14653240903219122.
45. WJ J, RJ K, Ra B, MJ R, Mn H. Rapid attachment of adipose stromal cells on resorbable polymeric scaffolds facilitates the one-step surgical procedure for cartilage and bone tissue engineering purposes. J Orthop Res. 2011;29(6):853–60. doi:10.1002/jor.21314.
46. Chan CKF, Gulati GS, Sinha R, Tompkins JV, Lopez M, Carter AC, Ransom RC, Reinisch A, Wearda T, Murphy M. Identification of the human skeletal stem cell. Cell. 2018;175(1):43–56 e21. doi:10.1016/j.cell.2018.07.029.
47. Singh A, Gill G, Kaur H, Amhmed M, Jakhu H. Role of osteopontin in bone remodeling and orthodontic tooth movement: a review. Prog Orthod. 2018;19(1):18. doi:10.1186/s40510-018-0216-2.
48. Rosset EM, Bradshaw AD. SPARC/osteonectin in mineralized tissue. Matrix Biol. 2016;52-54:78–87. doi:10.1016/j.matbio.2016.02.001.
49. Veillette CJ, von Schroeder HP. Endothelin-1 down-regulates the expression of vascular endothelial growth factor-A associated with osteoprogenitor proliferation and differentiation. Bone. 2004;34(2):288–96. doi:10.1016/j.bone.2003.10.009.
50. Hu K, Olsen BR. Vascular endothelial growth factor control mechanisms in skeletal growth and repair. Dev Dynam. 2017;246(4):227–34. doi:10.1002/dvdy.24463.
51. Ma J, Both SK, Yang F, Cui FZ, Pan J, Meijer GJ, Jansen JA, Beucken JJJPVD. Concise review: cell-based strategies in bone tissue engineering and regenerative medicine. Stem Cells Transl Med. 2014;3(1):98–107. doi:10.5966/sctm.2013-0126.
52. Kook YM, Jeong Y, Lee K, Koh WG. Design of biomimetic cellular scaffolds for co-culture system and their application. J Tissue Eng. 2017;8:2041731417724640. doi:10.1177/2041731417724640.
53. Zimta AA, Baru O, Badea M, Buduru SD, Berindan-Neagoe I. The role of angiogenesis and pro-angiogenic exosomes in regenerative dentistry. Int J Mol Sci. 2019;20(2):406. doi:10.3390/ijms20020406.
54. Li Z, Yang A, Yin X, Dong S, Luo F, Dou C, Lan X, Xie Z, Hou T, Xu J. Mesenchymal stem cells promote endothelial progenitor cell migration, vascularization, and bone repair in tissue-engineered constructs via activating CXCR2-Src-PKL/Vav2-Rac1. Faseb J. 2018;32(4):2197–211. doi:10.1096/fj.201700895R.
55. Pill K, Melke J, Mühleder S. Microvascular networks from endothelial cells and mesenchymal stromal cells from adipose tissue and bone marrow: a comparison. Front Bioeng Biotechnol. 2018;6:156. doi:10.3389/fbioe.2018.00156.
56. Souilhol C, Serbanovic-Canic J, Fragiadaki M, Chico TJ, Ridger V, Roddie H, Evans PC. Endothelial responses to shear stress in atherosclerosis: a novel role for developmental genes. Nat Rev Cardiol. 2020;17(1):52–63. doi:10.1038/s41569-019-0239-5.
57. Potter CM, Lao KH, Zeng L, Xu Q. Role of biomechanical forces in stem cell vascular lineage differentiation. Arterioscler Thromb Vasc Biol. 2014;34(10):2184–90. doi:10.1161/ATVBAHA.114.303423.
58. Dan P, Velot E, Decot V, Menu P. The role of mechanical stimuli in the vascular differentiation of mesenchymal stem cells. J Cell Sci. 2015;128:2415–22. doi:10.1242/jcs.167783.
59. Kumar D, Cain SA, Bosworth LA. Effect of topography and physical stimulus on hMSC phenotype using a 3D in vitro model. Nanomaterials (Basel). 2019;9(4):522. doi:10.3390/nano9040522.

60. Liu X, Jakus AE, Kural M, Qian H, Engler A, Ghaedi M, Shah R, Steinbacher DM, Niklason LE. Vascularization of natural and synthetic bone scaffolds. Cell Transplant. 2018;27(8):1269–80. doi:10.1177/0963689718782452.
61. Chen CL, Guo HR, Wang YJ, Chang HT, Pan CY, Tuan-Mu HY, Lin HC, Chen CY, Hu JJ. Combination of inductive effect of lipopolysaccharide and in situ mechanical conditioning for forming an autologous vascular graft in vivo. Sci Rep. 2019;9(1):10616. doi:10.1038/s41598-019-47054-2.
62. Dang M, Saunders L, Niu X, Fan Y, Ma PX. Biomimetic delivery of signals for bone tissue engineering. Bone Res. 2018;6:25. doi:10.1038/s41413-018-0025-8.
63. Baumgartner W, Otto L, Hess SC, Stark WJ, Marsmann S, Burgisser GM, Calcagni M, Cinelli P, Buschmann J. Cartilage/bone interface fabricated under perfusion: spatially organized commitment of adipose-derived stem cells without medium supplementation. J Biomed Mater Res B. 2018;107(6):1833–43. doi:10.1002/jbm.b.34276.
64. Nguyen BN, Ko H, Moriarty RA, Etheridge JM, Fisher JP. Dynamic bioreactor culture of high volume engineered bone tissue. Tissue Eng Part A. 2016;22(3–4):263–71. doi:10.1089/ten.tea.2015.0395.